

Electronic and Geometric Structure of the Titanium Hydrides, TiH^+ and TiH_2^+

Aristides Mavridis*

Department of Chemistry, University of Athens, 13A Navarinou Street, Athens 10680, Greece

James R. Harrison

Department of Chemistry, Michigan State University, East Lansing, Michigan 48824-1322, U.S.A.

The electronic and geometric structures of TiH^+ and TiH_2^+ have been studied by *ab initio* MCSCF and MCSCF-CI techniques. The ground state of TiH^+ is $^3\Phi$, but within 2 kcal mol⁻¹, three states $^2\text{B}_1$, $^2\text{A}_2$ and $^2\text{A}_1$ compete for the ground state of the TiH_2^+ cation. At the MCSCF+1+2 level, the $^2\text{A}_1$ potential-energy surface with respect to the HTiH angle presents two almost symmetrically located energy minima with an energy barrier between them of ca. 1.3 kcal mol⁻¹.

Recently, there has been a surge of interest in the gas-phase chemistry of transition-metal elements with small organic and inorganic molecules. *Ab initio* quantum-chemical techniques provide an excellent tool especially suited for small systems in the gas phase, and it would be profitable¹ to study the experimental data already in existence with a view to interpreting trends.^{2,3}

The purpose of the present study is to obtain structural information on the cations TiH^+ , TiH_2^+ and to speculate about the energetics of the reaction, $\text{TiH}_2^+ \rightarrow$ products.

Basis Sets and Molecular Codes

The basis set for the Ti atom is Wachters's⁴ 14s9p5d one-electron Gaussian basis augmented with two additional p functions,⁵ to represent the 4p space and an extra d function as recommended by Hay.⁶ The resulting 14s11p6d primitive set was contracted to [5s4p3d] according to Raffanetti.⁷ The hydrogen atom basis was the 4s Huzinaga basis,⁸ augmented by a set of p polarization functions with an exponent of 1.0. The resulting 4s1p basis set was contracted to [2s1p] according to Raffanetti.⁷ The final basis set contains 37 and 42 contracted Gaussians for TiH^+ and TiH_2^+ , respectively. Our experience with the previously described basis concerning the first half of the first-row transition-metal elements for a variety of chemical systems is quite good.^{2,9,10}

All calculations were performed on an FPS-164 jointly supported by the Michigan State University Chemistry Department and the office of the Provost, using the Argonne National Laboratory collection of QUEST-164 codes.

Results and Discussion

The TiH^+ System

The ground state¹¹ of the Ti^+ ion is a ^4F state which comes from a $4\text{d}^24\text{s}^1$ valence configuration. A ^4P state¹¹ which arises from the same configuration is 1.21 eV above the ^4F ground state (average over M_J values). At the SCF level we compute a $\Delta E_{4\text{F}-4\text{P}} = 1.29$ eV, in good agreement with the experimental value.

As the H atom in its ^2S ground state approaches the Ti^+ ion along the Z axis, four low-lying states (triplets or singlets) are possible, owing to the breaking of spherical symmetry: Σ , Π , Δ and Φ . We find, in agreement with recently published calculations on charged monohydrides,^{3,12,13} that the ground state is $^3\Phi$. Here we focus our attention on this $^3\Phi$ ground state. The most chemically intuitive way to understand the bonding in this system is to imagine the 4s electron of the metal to be coupled in a valence-bond fashion with the oncoming 1s electron of the hydrogen atom. Thus, our simplest description of the bond formation between Ti^+ and $\text{H}(^2\text{S})$ is described by a GVB-PP(1/2) function^{14,15} with the two non-bonding d electrons triplet-coupled:

$$^3\Phi = (\text{Ar})(\sigma h + h\sigma)d_\pi d_{\Delta-}(\alpha\beta + \beta\alpha)\alpha\alpha \quad (1)$$

where, at large interatomic distances, σ and h represent the 4s orbital on Ti^+ and the hydrogen 1s function, respectively. Because the calculations are done under C_{2v} symmetry $d_{\Delta-}$ is an orbital of a_2 symmetry. $(\text{Ar}) \equiv (1s)^2(2s)^2(2p)^6(3s)^2(3p)^6$. This GVB (generalized valence bond,¹⁵ *i.e.* a traditional Heitler-London function with the relevant bonding orbitals self-consistently optimized), describes the (assumed) single bond accurately enough, taking into account the left-right correlation of the bond and separating in many cases to the ground, SCF states, of the two fragments. However, in the present case, owing to the character of the *in situ* description of the Ti^+ atom in the $^3\Phi$ ground state, the Ti^+ ion at infinity is described by the mixture $2/\sqrt{5}|^4\text{F}\rangle - 1/\sqrt{5}|^4\text{P}\rangle$, which is 0.0185 hartree higher than the ^4F pure state. Of course this is taken into account in calculating the dissociation energy by this method. If we replace the GVB description by an essentially equivalent MCSCF function consisting of all configuration state functions (CSFs)¹⁶ of Φ symmetry arising from three active orbitals of σ symmetry and two of π and $d_{\Delta-}$ symmetry (the last two being triplet-coupled and always singly occupied) we have in C_{2v} symmetry five CSFs. The dissociation curve (D) versus the interatomic distance (R) calculated from this MCSCF function is shown in fig. 1, along with the MC-CI results generated from all single and double excitations from this five-configuration reference space (MCSCF+1+2, 1510 CSFs).

In table 1 we have collected all our pertinent numerical results in all three different methods used in this study. For comparison, the results of two different studies published recently^{3,12,13} are also included. Although the geometry (R_e) and the vibrational frequency (ω_e) obtained from the MCSCF+1+2 results of the present study are in good agreement with the previously reported results^{3,12,13} (table 1), the following observations are in order. At the MCSCF+1+2 level we extract much more correlation energy associated with the 4s and 3d orbitals compared with the GVB-DCCI calculations. In the light of this, we think that the perfect agreement between the experimental dissociation energy, D_0 ,¹⁷ and that calculated by the GVB-DCCI method^{12,13} is somewhat fortuitous. The MCPF technique^{18,19} is a single reference +1+2 CI (CISD) which takes into account unlinked clusters; it is size consistent but not variational. Results obtained with the MCPF method are in very good agreement with experiment.³ The reported³ result in table 1 concerning D_0 (the only experimental results available for TiH^+) strengthens this claim. Our reported D_0 value can only be considered in fair agreement with the experiment. Notice, that the MCSCF+1+2 calculations are practically size constant,⁶ particularly in this case where the number of active electrons is only four.

Finally, from the Mulliken²⁰ population analysis, as obtained from the GVB-PP wavefunction (table 1), we find that at R_e the Ti^+ ion retains almost all of its charge and that the character of the Ti-H bond is a mixture of *ca.* 45% s, *ca.* 15% p and *ca.* 40% d orbitals in agreement with previous results.^{3,12,13}

The TiH_2^+ System

TiH_2^+ ion has five valence electrons. Constraining TiH_2^+ to have C_{2v} symmetry with the metal at the origin, the Z axis (a_1) being the symmetry C_2 axis, and defining the molecular

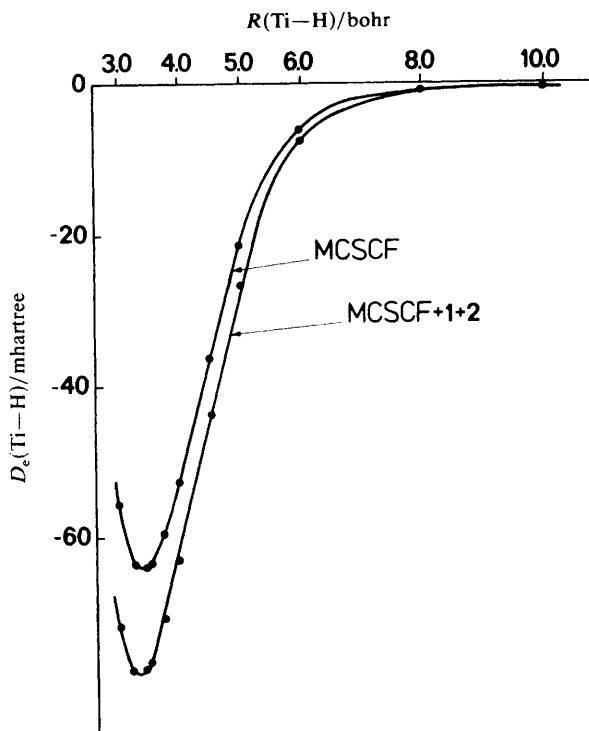


Fig. 1. Binding energy, D_e , of TiH^+ in the $^3\Phi$ state as a function of the distance $R_{\text{Ti-H}}$, in both the MCSCF and MCSCF+1+2 level of calculations. Note that the zero level of the MCSCF curve has been shifted to lower energy by 11.7 mhartree.

Table 1. Energies (E_e), equilibrium bond distances (R_e), vibrational frequencies (ω_e) and dissociation energies (D_e , D_0), of TiH^+ in the $^3\Phi$ electronic state

method	$E_e/\text{hartree}$	$R_e/\text{\AA}$	ω_e/cm^{-1}	$D_e/\text{kcal mol}^{-1}$	$D_0/\text{kcal mol}^{-1}$
GVB-PP(1/2) ^a	-848.741 02	1.796	1563	32.8	
MCSCF ^a	-848.741 62	1.797	1558	33.2	
MCSCF+1+2 ^a	-848.770 33	1.755	1643	58.9	46.6
GVB-DCCI ^b	-847.827 88	1.73	1696	56.4	54.0
MCPF ^c		1.740	1705		51.0
exptl ^d					55.1 ± 2

^a This study. ^b GVB-dissociation consistent CI¹⁵, results from ref. (12), (13). The GVB-PP energy reported in ref. (13), as well as the GVB-DCCI energy, are more than 0.9 hartree higher than our GVB-PP energy which reflects on the energetics of the ^4F atom: for the ^4F of Ti^+ we calculate an energy -848.189 46 hartree, consistent with that of ref. (4), while the corresponding GVB energy of ref. (13) is -847.238 03 hartree, a difference of ca. 0.95 hartree. Considering that the two basis sets used are essentially equivalent, we cannot account for this discrepancy. ^c Modified couple pair formalism,¹⁹ results from ref. (3), no energies are reported. ^d Ref. (17).

Table 2. SCF equilibrium energies, equilibrium bond angles (θ_e) and dissociation energies (D) of TiH_2^+ in various states

state ^a	E_e /hartree	θ_e ^b /°	D_e ^c /kcal mol ⁻¹
2A_2	-849.2247	97	22.6
2B_2	-849.1840	180	-2.8
2A_1	-849.2318	120	27.2
2B_1	-849.2333	120	28.1

^a States 2A_2 , 2B_2 are the two ${}^2\Pi$ components of the linear symmetry ($\theta = 180^\circ$); 2A_1 and 2B_1 are the ${}^2\Delta$ components. ^b $R_{\text{Ti-H}}$ fixed at 3.30 bohr (= 1.746 Å). ^c With respect to $\text{Ti}^+(\text{F}) + 2\text{H}(\text{S})$.

plane to be $YZ(b_2)$ the Ar 18-electron core has the description:

$$(\text{core}) = 1a_1^2 2a_1^2 3a_1^2 4a_1^2 5a_1^2 1b_1^2 2b_1^2 1b_2^2 2b_2^2.$$

The two Ti—H bonds are of $6a_1$ and $3b_2$ symmetry and the non-bonding electron which defines the overall symmetry can be allotted to any of the four representations of the C_{2v} group. Therefore, in principle, four low-lying doublets are feasible, 2A_1 , 2A_2 , 2B_1 and 2B_2 with the following Hartree-Fock description:

$$(\text{core})6a_1^2 3b_2^2 \begin{cases} a_1^1 \alpha \beta \alpha \beta \alpha = {}^2A_1 \\ a_1^2 \alpha \beta \alpha \beta \alpha = {}^2A_2 \\ b_1^1 \alpha \beta \alpha \beta \alpha = {}^2B_1 \\ b_1^2 \alpha \beta \alpha \beta \alpha = {}^2B_2 \end{cases}$$

As it turns out, the 2A_1 , 2A_2 and 2B_1 states are degenerate within the resolving power of our computations. 2B_1 is formally the ground state, while 2B_2 is 43.9 kcal mol⁻¹ above the 2B_1 state [in the energy diagrams we use mhartree (= 0.627 51 kcal mol⁻¹)]. Qualitatively, the energy location of the four states is not unexpected: avoiding the bonding electron densities, the non-bonding electron would rather occupy the a_2 or b_1 symmetry blocks, being in both cases perpendicular to the molecular plane. The fact that the 2B_2 state is much higher than the 2A_1 state can be attributed to the fact that the a_1 symmetry orbital block is much more flexible than b_2 . In table 2, we present the SCF equilibrium energies and angles ($\theta_e = \angle \text{HTiH}$), while keeping the bond distances fixed at $R = 3.30$ bohr (= 1.746 Å), *i.e.* close to the Ti—H bond distance in the ${}^3\Phi$ state (table 1). With the exception of the 2B_2 state this bond distance is close to the equilibrium distance (*vide infra*). The SCF results, table 2, are given not so much for the chemical information they convey but rather as a reference point. Correlating the two bonds in a GVB-PP(2/4) fashion^{14,15} we would write for instance for the 2A_2 state:

$${}^2A_2(\text{GVB-PP}) = (\text{core})(6a_1^2 - \lambda 7a_1^2)(3b_2^2 - \mu 4b_2^2)a_2^1 \alpha \beta \alpha \beta \alpha. \quad (2)$$

Eqn. (2) is the natural orbital form of the GVB wavefunction; $\lambda, \mu > 0$, and if $\lambda = \mu = 0$ the SCF description obtains. The 2B_2 , 2A_1 and 2B_1 states are clearly obtained from eqn (2) by changing the occupation of the (spatial) symmetry-carrying orbital a_2 to the symmetries b_2 , a_1 and b_1 .

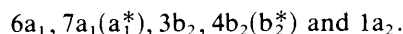
We obtain a better description than the GVB 19 CSFs MCSCF description by allotting the five valence electrons among five orbitals and allowing for the appropriate spin couplings, at the same time keeping the symmetry-defining orbital singly occupied. For

Table 3. MCSCF and MCSCF + 1 + 2 equilibrium energies (E_e), bond distances (R_e) and bond angles (θ_e) as obtained from the surface optimization of TiH_2^+ in four states

state	CSFs ^a	E_e /hartree	R_e /bohr (Å)	$\theta_e/^\circ$
MCSCF				
$^2\text{A}_2$	19	-849.2860	3.267 (1.729)	76.6
$^2\text{B}_2$	19	-849.2189	3.381 (1.789)	180
$^2\text{A}_1$	19	-849.2883	3.31 (1.75)	83 ^b
$^2\text{B}_1$	19	-849.2884	3.28 (1.74)	106.2
MCSCF + 1 + 2				
$^2\text{A}_2$	8578	-849.3237	3.23 (1.71)	72.6
$^2\text{B}_2$	9501	-849.2552	3.357 (1.776)	180 ^b
$^2\text{A}_1$	9526	-849.3228	3.23 (1.71)	61 ^b
$^2\text{B}_1$	8588	-849.3252	3.23 (1.71)	107.0

^a Number of configuration state functions.¹⁶ ^b See text.

the $^2\text{A}_2$ state, for instance, the following five orbitals define the valence space:

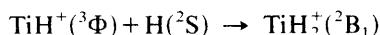


The correspondence with the GVB-PP description is obvious.

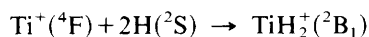
To improve upon the MCSCF-19CSFs wavefunction we have constructed the MR-CI descriptions, *i.e.* MCSCF + 1 + 2 wavefunctions for all four states, and we have optimized the geometry of the system in both MCSCF and MCSCF + 1 + 2 schemes.

Table 3 gives a condensed presentation of our results. A first glance reveals that the $^2\text{A}_2$, $^2\text{A}_1$ and $^2\text{B}_1$ states are very close in energy, with $^2\text{B}_1$ being the ground state and lower in energy than $^2\text{B}_2$ by 43.9 kcal mol⁻¹. Note that $^2\text{B}_1$ is calculated to be the lowest state in all levels of calculations, even SCF. The MCSCF brings the $^2\text{A}_2$ and $^2\text{A}_1$ states closer together, but still retains the order of the SCF. The MCSCF + 1 + 2 flips the two levels so that $^2\text{A}_2$ becomes the lower of the two states by *ca.* 0.6 kcal mol⁻¹.

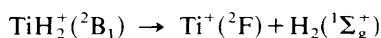
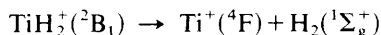
Fig. 2 shows the energetics of the reaction $\text{TiH}_2^+ \rightarrow$ products at the MCSCF + 1 + 2 level of calculation. The following conclusions can be inferred. The reaction



(or for that matter any of the states $^2\text{B}_1$, $^2\text{A}_2$, $^2\text{A}_1$) is exothermic by 34.7 kcal mol⁻¹, while the reaction



is exothermic by 83.5 kcal mol⁻¹. On the other hand, the two reactions



are exothermic by *ca.* 20 kcal mol⁻¹ and *ca.* 16 kcal mol⁻¹, respectively. The first is spin-forbidden but the second is not, so once TiH_2^+ is formed it can easily dissociate on the $\text{Ti}(^2\text{F}) + \text{H}_2(^1\Sigma_g^+)$ surface. The direct leaking of TiH_2^+ to the $\text{Ti}^+(^4\text{F}) + \text{H}_2(^1\Sigma_g^+)$ surface is also plausible through spin-orbit coupling, but the first channel is more efficient.

Fig. 3 shows the MCSCF angular energy dependence curves for all four states. The third dimension of those surfaces, *i.e.* the Ti—H bond distance has been fixed to 3.30 bohr.

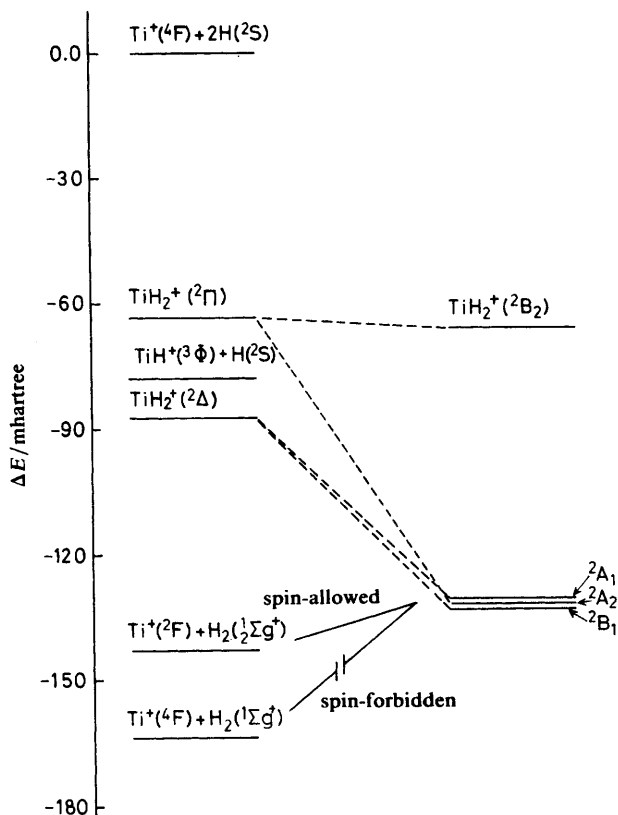


Fig. 2. Energetics of the system $\text{TiH}_2^+ \rightarrow \text{products}$ at the MCSCF+1+2 level.

As the molecule opens up, eventually becoming linear and lying along the Y axis, the ${}^2\text{A}_1$, ${}^2\text{B}_2$ and ${}^2\text{A}_1$, ${}^2\text{B}_1$ states converge to the doubly degenerate ${}^2\Pi$ and ${}^2\Delta$ states, respectively (fig. 3). The ${}^2\text{A}_1$ surface is extremely floppy, thus rendering the determination of a single θ_e value almost lacking in physical meaning. In table 3, the value reported, 83° , is the mid-point of the flat portion of the ${}^2\text{A}_1$ curve. At the MCSCF+1+2 level the topology of the ${}^2\text{A}_2$ and ${}^2\text{B}_1$ surfaces ($R_{\text{Ti-H}} = 3.30$ bohr) remains the same, but that of the ${}^2\text{B}_2$ and ${}^2\text{A}_1$ surfaces changes (fig. 4). The flat portion of the ${}^2\text{A}_1$ surface at the MCSCF level (fig. 4) develops two minima at *ca.* 60° and *ca.* 120° , with an energy barrier between them of *ca.* 1.3 kcal mol $^{-1}$. We can envisage that the molecule in that state can find itself in any of these minima, rolling easily from one to the other. An energy barrier of 1.3 kcal mol $^{-1}$ is close to or smaller than the zero-point energy of the system. The ${}^2\text{B}_2$ surface, on the other hand, at the MCSCF+1+2 level develops a shallow minimum around 160° instead of 180° (${}^2\Pi$) which was the MCSCF (and SCF) value. The energy at 160° is *ca.* 3 kcal mol $^{-1}$ lower than that of the corresponding linear geometry. This could be an artefact due to the basis set. In table 3 the reported optimized Ti—H bond distances of the ${}^2\text{B}_2$ and ${}^2\text{A}_1$ states correspond to θ values of 180° and 61° respectively.

Alvarado-Swaisgood and Harrison²¹ carried out similar calculations on the ScH_2^+ ${}^1\text{A}_1$ (ground) state. Assuming that the two systems $\text{TiH}_2^+({}^2\text{B}_1)$ and $\text{ScH}_2^+({}^1\text{A}_1)$ have similar bonding character (they differ by a single electron added to the closed-shell system of ScH_2^+ in a symmetry which does not interfere with the bonding), a comparison between the two is appropriate. At the MCSCF+1+2 level and with an identical basis

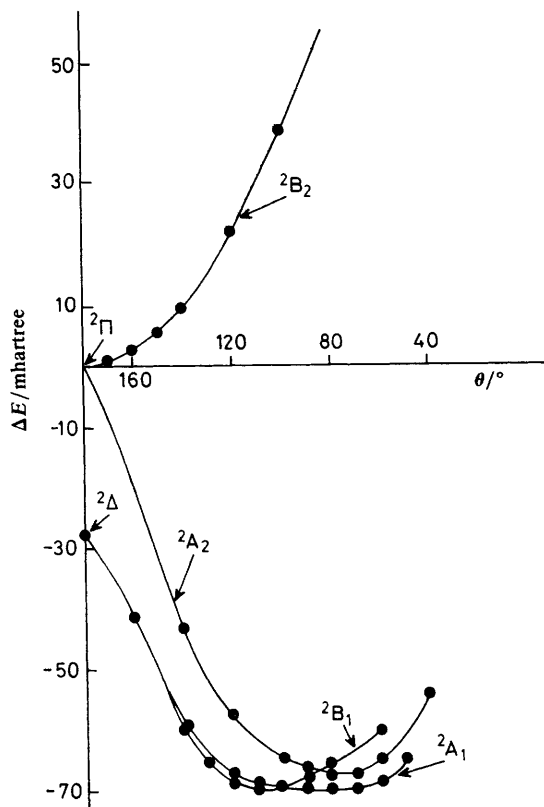


Fig. 3. Dependence of the TiH_2^+ total energy in the ${}^2\text{B}_1$, ${}^2\text{A}_1$ and ${}^2\text{B}_2$, ${}^2\text{A}_2$ states at the MCSCF level as a function of the $\text{HTiH}(\theta)$ angle. The Ti—H bond distance has been fixed at 3.30 bohr (1.746 Å), *i.e.* the equilibrium bond distance found for $\text{TiH}^+({}^3\Phi)$.

set with ours (spd), Alvarado-Swaisgood and Harrison²¹ obtained $R_e = 1.757$ Å and $\theta_e = 103.6^\circ$ for ScH_2^+ , values not very different from those of $\text{TiH}_2^+({}^2\text{B}_1)$ (table 3). They also reported²¹ a D_e value of 106.4 kcal mol⁻¹ with respect to $\text{Sc}^+({}^3\text{D}) + 2\text{H}({}^2\text{S})$, using a basis set augmented by a single set of f functions [spdf set in ref. (21)] on the metal. From results on $\text{ScH}^+({}^2\Delta)$ ² the effect of f functions on D_e is *ca.* 4 kcal mol⁻¹, therefore the D_e value of ScH_2^+ should be very close to 100 kcal mol⁻¹ in the spd basis set. This number should be contrasted to our D_e value of 83.5 kcal mol⁻¹ (fig. 2), with respect to $\text{Ti}^+({}^4\text{F}) + 2\text{H}({}^2\text{S})$. In addition, the reaction $\text{Ti}^+({}^4\text{F}) + \text{H}({}^2\text{S}) \rightarrow \text{TiH}^+({}^3\Phi)$ is exothermic by 48.9 kcal mol⁻¹ (D_e , table 1). The bonding of a second hydrogen to TiH^+ increases the exothermicity by 34.6 kcal mol⁻¹. The corresponding numbers for $\text{ScH}^+({}^2\Delta)$ and $\text{ScH}_2^+({}^1\text{A}_1)$ are 50.7 and *ca.* 50 kcal mol⁻¹. In the light of the above discussion we can qualitatively describe the bonding in $\text{TiH}_2^+({}^2\text{B}_1)$ as primarily due to hybridized Ti 4s and 3d_{yz} atomic orbitals which then interact with the incoming hydrogen atoms, quite similar to those of the ScH_2^+ system.²¹

Schilling *et al.*²² recently reported *ab initio* GVB calculations on the dihydrides CrH_2^+ and MoH_2^+ , both with a reported ${}^4\text{B}_2$ ground state. Their basis set for the Cr^+ ion is of a similar quality to ours, but for Mo^+ the Ni core was replaced by an *ab initio* core potential.²² At the GVB-RCI(2/4)¹⁵ level they obtained an HCrH angle of 107.5° and a Cr—H bond length of 1.635 Å. Note, though, that their angular energy diagram, ΔE versus $\theta(\text{HCrH})$ [fig. 2 of ref. (22)], is very similar to that of $\text{TiH}_2^+({}^2\text{A}_1)$ at the MCSCF

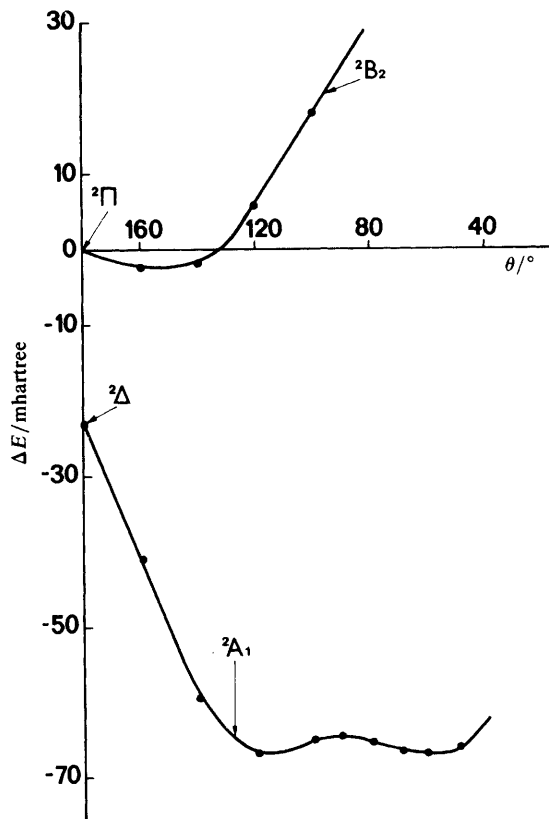


Fig. 4. Dependence of the TiH_2^+ total energy in the 2A_1 and 2B_2 states at the MCSCF+1+2 level as a function of the $\text{HTiH}(\theta)$ angle. The Ti—H bond distance is fixed at 3.30 bohr. Two minima are found at ca. 60 and ca. 120° with an energy barrier of ca. 1.3 kcal mol⁻¹.

level (fig. 2), the flat portion of the $\langle \text{HCrH} \rangle$ curve ranging from 70 to 120°. The MoH_2^+ angular energy diagram [fig. 4 of ref. (22)] at the GVB-RCI(2/4) level, is strikingly similar to that of TiH_2^+ 2A_1 state at the MCSCF+1+2 level (fig. 4). Schilling *et al.*²² report two distinct minima at θ values of 65 and 112°, with a barrier between them at 88°, of energy less than 1.5 kcal mol⁻¹. As already reported, our two distinct minima occur at 61 and 120° with an energy barrier of ca. 1.3 kcal mol⁻¹ at ca. 90° (fig. 4).

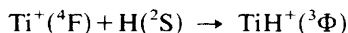
Conclusion

(a) The ground state of TiH^+ is of ${}^3\Phi$ symmetry with a calculated D_0 of 46.6 kcal mol⁻¹, in reasonable agreement with the experimental value of 55.1 ± 2 kcal mol⁻¹.

(b) The (formal) ground state of TiH_2^+ is of 2B_1 symmetry with two states, 2A_2 and 2A_1 , just ca. 0.95 and ca. 1.5 kcal mol⁻¹ higher. A fourth state, 2B_2 , is above the 2B_1 state by as much as 44 kcal mol⁻¹. At the 2B_1 symmetry TiH_2^+ has an equilibrium geometry of $\theta_e = 107.0^\circ$ and $R_{\text{Ti-H}} = 1.71 \text{ \AA}$; this geometry is very similar to that of $\text{ScH}_2^+({}^1A_1)$.

(c) The bonding character is due mainly to 4s3d hybridization and overlap with the 1s orbitals of hydrogen atoms.

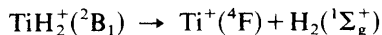
(d) The reactions



and



are strongly exothermic with an average bond strength of *ca.* 42 kcal mol⁻¹, while the reactions



and



are exothermic (the former being spin-forbidden and the latter spin-allowed) with exothermicities of *ca.* 20 and 16 kcal mol⁻¹, respectively.

Although in fig. 2 we indicate that depending on the spin of the metal, the lowest-energy products of the reaction $\text{TiH}_2^+ \rightarrow$ products are either $\text{Ti}^+(^2\text{F}) + \text{H}_2(^1\Sigma_{g+})$ or $\text{Ti}^+(^4\text{F}) + \text{H}_2(^1\Sigma_g^+)$, in reality the lowest-energy product will be a weakly bound electrostatic complex of the form $\text{Ti}^+ \cdots \begin{array}{c} \text{H} \\ | \\ \text{H} \end{array}$. At a Ti—H₂ distance of *ca.* 2 Å, this T-shaped complex has a binding energy²³ of *ca.* 4 kcal mol⁻¹. Interestingly enough, in this system the spin symmetry of the metal ion is the spin of $\text{Ti}^+ \cdots \begin{array}{c} \text{H} \\ | \\ \text{H} \end{array}$.

(e) The ²A₁ surface of TiH₂⁺ at the MCSCF+1+2 level of calculation presents two, almost symmetrical, distinct minima with an energy barrier of *ca.* 1.3 kcal mol⁻¹ at *ca.* 90°. The topology of this surface is in striking similarity with that of MoH₂⁺(⁴B₂).

References

- 1 E. R. Davidson, *Faraday Symp. Chem. Soc.*, 1984, **19**, 7.
- 2 A. E. Alvarado-Swaisgood and J. F. Harrison, *J. Phys. Chem.*, 1988, **92**, 2757 and references therein.
- 3 L. G. M. Pettersson, C. W. Bauschlicher Jr, S. R. Langhoff and H. Partridge, *J. Chem. Phys.*, 1987, **87**, 481 and references therein.
- 4 A. J. H. Wachters, *J. Chem. Phys.*, 1970, **82**, 1033.
- 5 T. K. Dunning Jr, personal communication.
- 6 P. Hay, *J. Chem. Phys.*, 1977, **66**, 4377.
- 7 R. C. Raffanetti, *J. Chem. Phys.*, 1973, **58**, 4452.
- 8 S. Huzinaga, *J. Chem. Phys.*, 1965, **42**, 1293.
- 9 A. Mavridis, A. E. Alvarado-Swaisgood and J. F. Harrison, *J. Phys. Chem.*, 1986, **90**, 2584.
- 10 A. Mavridis, J. F. Harrison and J. Allison, *J. Am. Chem. Soc.*, 1989, **111**, 2482.
- 11 C. E. Moore, *Atomic Energy Levels* (National Bureau of Standards, Washington D.C., 1971), vol I.
- 12 J. B. Schilling, W. A. Goddard III and J. L. Beauchamp, *J. Am. Chem. Soc.*, 1986, **108**, 582.
- 13 J. B. Schilling, W. A. Goddard III and J. L. Beauchamp, *J. Phys. Chem.*, 1987, **91**, 5616.
- 14 F. B. Bobrowitz and W. A. Goddard III., in *Modern Theoretical Chemistry: Methods and Electronic Structure Theory*, ed. H. F. Schaeffer III (Plenum Press, New York, 1977), vol. 3.
- 15 E. A. Carter and W. A. Goddard III, *J. Chem. Phys.*, 1988, **88**, 3132 and references therein.
- 16 H. Lischka, R. Shepard, F. B. Brown and I. Shavitt, *Int. J. Quantum Chem. Symp.*, 1981, **15**, 91.
- 17 J. L. Elkind and R. B. Armentrout, *Inorg. Chem.*, 1986, **25**, 1080.
- 18 R. Ahlrichs, P. Scharf and C. Ehrhardt, *J. Chem. Phys.*, 1985, **82**, 890.
- 19 D. P. Chong and S. R. Langhoff, *J. Chem. Phys.*, 1986, **84**, 5006.
- 20 R. S. Mulliken, *J. Chem. Phys.*, 1955, **23**, 1833; 1841; 2338; 2343. For a critique see: J. O. Noel, *Inorg. Chem.*, 1982, **21**, 11.
- 21 A. E. Alvarado-Swaisgood and J. F. Harrison, *J. Phys. Chem.*, 1985, **89**, 5198.
- 22 J. B. Schilling, W. A. Goddard III and J. L. Beauchamp, *J. Phys. Chem.*, 1987, **91**, 4470.
- 23 A. Mavridis and J. F. Harrison, unpublished results.